

## MPS SIMULATION OF NATURAL CONVECTION WITH INTERNAL HEATING IN A CAVITY

Tatsuya Kawaguchi

Tokyo Institute of Technology.  
Graduate school of mechanical and control engineering  
Ookayama 2-12-1 Meguroku, Tokyo Japan  
e-mail: kawat@mep.titech.ac.jp url: <http://netsu-n.mep.titech.ac.jp/>

**Key words:** Natural convection, Internal heating, Molten glass, Particle Method

**Abstract.** For the stable melting of the high temperature molten glass beyond 1200 degree Celsius, fluid motion and thermal energy balance due to the natural convection are the most important phenomena to control the state of the molten materials and blending process of the particulate materials. In the present study, the numerical simulation of natural convection flow by the conductive heat transfer in a rectangular cavity was investigated. Moreover the effect of the internal heating such as Joule heating was considered and compared, which was used in the engineering field of the development of the glass melting method for vitrified high-level radioactive waste. For the numerical analysis of the aforementioned flow field, the moving particle semi-implicit method was employed to predict the velocity distribution of the fluid flows as well as the temperature distribution. Mass, momentum and energy equation was used. Boussinesq approximation was applied to estimate the buoyancy force. Since the particle method we used is the meshless method, it is easy to compute the flow with free surface as well as the throwing of the additional fluid particles into the cavity. In the numerical analysis, Rayleigh number with internal heating was varied to compare the fluid behaviour, spatial distribution of temperature and the velocity magnitude of the downward plume.

### 1 Introduction

Natural convection with internal heating is the flow due to the temperature difference within the enclosure. In many applications, the energy source of the internal heating could be electric current for Joule heating, absorption of electromagnetic wave and such molecular or atomic reactions as chemical reactions and nucleosynthesis. For example, mantle convection is one of the applications of the natural convection with internal heating[1]. The Joule heating of high temperature molten glass is of our interest.

Stanek *et al.*[2] reported the first approach for the modelling of the electric melting of glass in furnaces and they employed not only Grashof number but also Galileo analogy for

the modelling of the convection of molten glass by electric heating. The group employed the glycerol as a working fluid with an addition of LiCl so that they could simulate the kinematic viscosity as well as the resistivity of model liquid with soda-lime-silica glass. They also investigated the location and orientation of the multiple electrodes, moreover the phase of the electric current was considered.

The numerical prediction and relevant experiments of the physics of a natural convection in a cavity has been investigated by many groups[3]-[7]. Liaquat and Baytas[8] have numerically investigated the heat transfer characteristics of internally heated square cavity at high Rayleigh numbers from  $10^7$  to  $10^{12}$ . They concluded that the flow pattern with lower Rayleigh number showed periodic oscillation whereas the higher Rayleigh number caused non-periodic time-dependent behaviour. Since the instability of the flow field is essentially present and the considerable range of  $Ra$  number is widely varied, the verification of each numerical model is complicated without the detailed and precise experimental data. The objective of the present study is to analyse a natural convection in a rectangular cavity with Joule heating by means of particle method.

In the actual glass melting furnaces, the electric conductivity of molten glass as well as the other physical properties such as viscosity, density and thermal conductivity are significantly affected by temperature. The electric conductivity of molten glass beyond  $1000^\circ\text{C}$  is as high as that of the semiconductor materials. The electric current through a molten glass is not due to the free electron but due to the ion in the high temperature glass. It must be noted that the electric conductivity of the electrolyte such as LiCl and KCl water solution is affected by the frequency in contrast to the frequency independency of the conductivity of molten glass[9, 10]. In the present numerical study, such electromagnetic effect as Lorentz force was ignored, only the internal heating source was considered as an electric Joule heating[11].

## 2 Numerical methods

In this section, the method of numerical analyses was described.

Flow is assumed to be incompressible and two-dimensional. Employing an incompressible continuous equation as follows;

$$\nabla \cdot \mathbf{v} = 0 \quad (1)$$

For the momentum equation, surface tension at free surface and any body forces except buoyancy were ignored due to the high viscosity of working fluid. Non-slip boundary condition was used at the liquid-solid interface.

$$\rho \frac{Dv_m}{Dt} = \frac{\partial}{\partial x_n} (-P\delta_{mn} + \tau_{mn}) + \rho g\beta(T - T_0) \quad (2)$$

In the momentum equation, Boussinesq approximation was used to estimate the buoyancy force.

Two-dimensional power law model was used for the constitution equation of the pseudoplastic fluid:

$$\tau_{mn} = \eta_0 |II_{2D}|^{\frac{n-1}{2}} (2D_{mn}) \quad (3)$$

$$II_{2D} = \frac{1}{2} ((tr 2D)^2 - tr(2D)^2) \quad (4)$$

$\eta_0$  and  $n$  are the constants depending on the rheological properties of fluid flow. The strain rate tensor,  $D$ , is expressed as follows;

$$D_{mn} = \frac{1}{2} \left( \frac{\partial v_m}{\partial x_n} + \frac{\partial v_n}{\partial x_m} \right) \quad (5)$$

For the thermal energy transportation, two-dimensional conductive heat transfer was applied.

$$\rho c_p \frac{DT}{Dt} = k \nabla^2 T + \dot{q} \quad (6)$$

Since the particle method employs the Lagrangian specification, the convection term is not appeared in the material derivative in the equation (6). Under the method, convective thermal transportation was considered as the explicit particle displacement in space. Assuming that the internal heating was homogeneously applied within a fluid, consequently the value of internal heat source,  $\dot{q}$ , was constant for the every fluid particle. The internal heating of the other particles such as solid wall were set to zero which represent no internal heating was applied for the solid materials.

## 2.1 Discretization method

We employed the moving particle semi-implicit method (MPS)[12] that is one of the meshless computation technique based on a simplified marker and cell (SMAC) method. The advantage of the method is that the arbitrary shaped gas-liquid surface could be easily expressed by the particle location that is treated as the free surface.

The following standard function was employed as a weighting function.

$$w(r) = \begin{cases} \frac{r_e}{r} - 1 & (0 < r \leq 1) \\ 0 & (r_e < r) \end{cases} \quad (7)$$

To compute the value of  $w$  during the computation,  $r_e = 2.1l_0$  for the gradient model,  $r_e = 4.0l_0$  for the Laplacian model were applied. Since the viscous force of non-Newtonian momentum equation could not be expressed by a conventional Laplacian models directly,

the deformation rate from the velocity distribution was firstly computed which was followed by the determination of the shear stress tensor by the constitutive equation.

To discretize the momentum equation, we divide the equation (2) into two parts as follows;

- viscous and buoyancy term

$$\mathbf{v}_m^* = \mathbf{v}_m^k + \Delta t \left\{ \frac{1}{\rho} \left( \frac{\partial \tau_{mn}}{\partial x_n} \right)^k + \mathbf{g} \beta (T^k - T_0) \right\} \quad (8)$$

- pressure gradient term

$$\mathbf{v}_m^{k+1} = \mathbf{v}_m^* - \frac{\Delta t}{\rho} \nabla P^{k+1} \quad (9)$$

Apply the gradient model of MPS to the right-hand side of equation (5) in order to calculate the rate of deformation around each particle.

$$2(D_{mn})_i^k = \left\langle \frac{\partial v_m}{\partial x_n} \right\rangle_i^k + \left\langle \frac{\partial v_n}{\partial x_m} \right\rangle_i^k \quad (10)$$

Calculate the second invariant of velocity gradient tensor, viscosity and deviatoric stress tensor.

$$(II_{2D})_i^k = \frac{1}{2} \left[ \{tr(2D_i^k)\}^2 - tr \{ (2D_i^k)(2D_i^k) \} \right] \quad (11)$$

$$\eta_i^k = \eta_0 \left| (II_{2D})_i^k \right|^{\frac{n-1}{2}} \quad (12)$$

$$(\tau_{mn})_i^k = \eta_i^k \cdot 2(D_{mn})_i^k \quad (13)$$

Apply the gradient model to the shear stress term in equation (8), estimate the temporal particle velocity,  $\mathbf{v}_m^*$ , and particle location,  $\mathbf{r}^*$ .

$$(\mathbf{v}_m)_i^* = (\mathbf{v}_m)_i^k + \Delta t \left\{ \frac{1}{\rho} \left\langle \frac{\partial \tau_{mn}}{\partial x_n} \right\rangle_i^k + \mathbf{g} \beta (T_i^k - T_0) \right\} \quad (14)$$

$$\mathbf{r}_i^* = \mathbf{r}_i^k + \Delta t \mathbf{v}_i^* \quad (15)$$

Calculate the number density distribution by using the updated particle positions.

$$n_i^* = \sum_{j \neq i} w(|\mathbf{r}_j^* - \mathbf{r}_i^*|) \quad (16)$$

Substitute the particle concentration into the Poisson equation of pressure to estimate the revised pressure,  $P^{k+1}$ , that homogenize the particle number concentration toward the initial value,  $n_0$ .

$$\langle \nabla^2 P \rangle_i^{k+1} = -\frac{\rho_0}{\Delta t^2} \frac{n_i^* - n^0}{n^0} \quad (17)$$

Finally, the amount of velocity correlation,  $\mathbf{v}'$ , by  $P^{k+1}$ , revise the velocity and position of every particles.

$$\mathbf{v}'_i = -\frac{\Delta t}{\rho} \langle \nabla^2 P \rangle_i^{k+1} \quad (18)$$

$$\mathbf{v}_i^{k+1} = \mathbf{v}_i^* + \mathbf{v}'_i \quad (19)$$

$$\mathbf{r}_i^{k+1} = \mathbf{r}_i^* + \Delta t \mathbf{v}'_i \quad (20)$$

The fundamental computation procedure of temporal progress was similar to the original MPS method. At the beginning of each time step, the arbitrary inter-particle distance were calculated and correlate the neighbouring particles. In the explicit part of the computation procedure, viscous and buoyant terms were firstly reflected that was followed by the implicit pressure calculation. Since the CPU time of such non-stationary solving technique as conjugate gradient method is not constant but depend on the matrix, the CPU times were estimated by averaging over several second of simulation time. The calculation of neighbouring particle table and solver for Laplace equation spent almost all time of computation.

In the computation code written in C++ used in the study, the particle class was defined that contains the physical quantities, *e.g.* neighbouring particle table, particle position, velocity, temperature, pressure and so on. Each particle object has a member function that compute the physical properties such as density, viscosity, thermal conductivity, specific heat and coefficient of volume expansion can be calculated as requested in the main program. Therefore the particle object could be easily and dynamically generated on the main memory. When the new particles were required at the arbitrary time step in the computation area under the situation that the fluid flow was incoming and/or outgoing from the region of interest, the dynamic allocation and/or destruction of particle object were simply applied.

### 3 Results and Discussion

Firstly, the conventional natural convection without internal heating was calculated with a rectangular open channel. The temperatures of solid surface were suddenly increased to the fixed value and liquid within a channel was heated by the thermal conduction. In the following prediction, radiative heat transfer was treated as the thermal

conductivity assuming that the spectral absorption coefficient of fluid was sufficiently large in the infrared region, in other word, the material was assumed to be optically thick[13]. Density, viscosity and thermal conductivity were varied as a function of temperature by noting the physical properties of borosilicate glass. Internal channel width and height was 0.57 m and 0.30 m respectively, depth of fluid, which corresponds to the characteristic length in the present study, was 0.15 m. Initial inter-particle separation was 8 mm, number of particle was 1300 approximately including the spatially-fixed solid surface. Kinematic viscosity was  $\nu = 0.01 \text{ m}^2/\text{s}$ , thermal diffusivity was  $\alpha = 2.26 \times 10^{-4} \text{ m}^2/\text{s}$ ,  $Pr$  and  $Gr$  were 44 and 783 respectively,  $Ra$  number was  $3.4 \times 10^4$ .

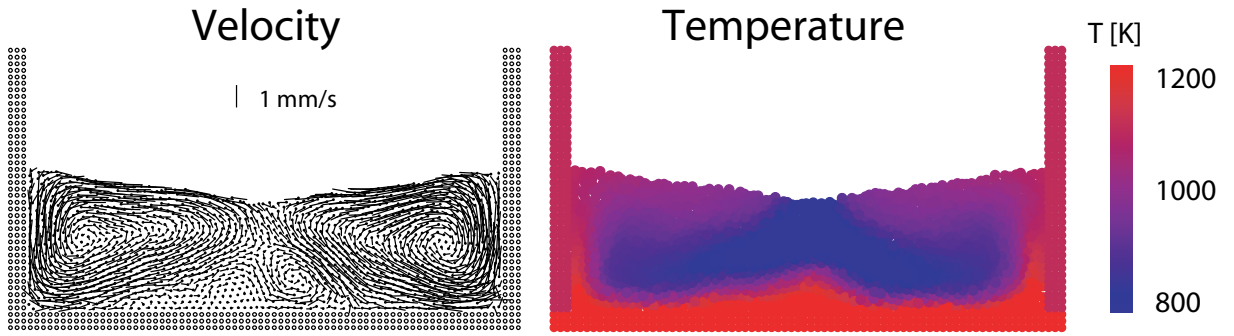


**Figure 1:** Velocity vector and temperature distribution of natural convection due to the heat transfer from the heated wall with constant temperature.

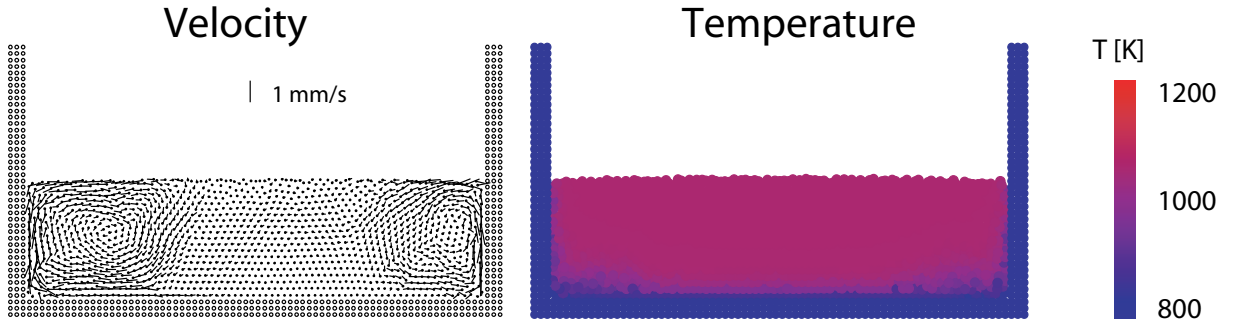
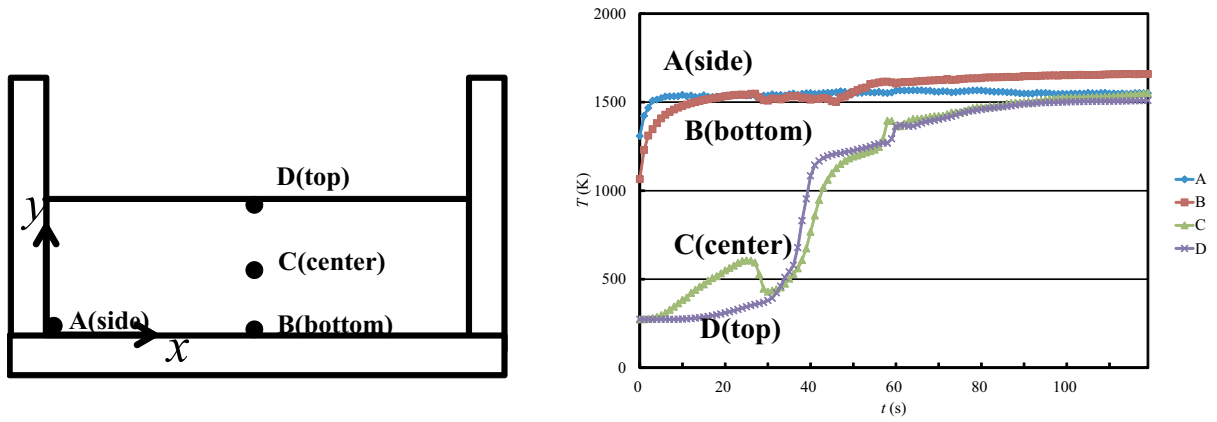


**Figure 2:** Velocity vector and temperature distribution of natural convection with internal heating.

Figure 1 depicts the examples of the velocity distribution in the channel as well as the temperature distribution at  $t = 20 \text{ s}$ . Initial temperature of each particle was 273.15 K, after the start of computation, the temperature of vertical and horizontal solid surface were kept constant at 1100 K and 1400 K respectively. At the beginning of heating, the upward flows with higher magnitude of velocity was induced in the vicinity of heated vertical surfaces due to the buoyancy force, and a pair of stable vortex was appeared. Simultaneously a plume was growing at the center of a channel by the conductive heat

transfer from the bottom surface. After the certain time, the velocity distribution as well as the temperature distribution becomes steady under the present configuration with four vortices.

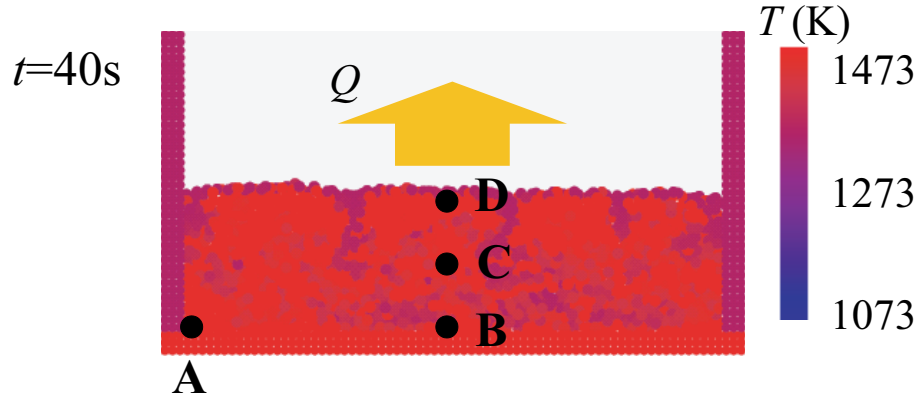
Figure 2 depicts the predicted results of natural convection with internal heating at  $t=37.5$  sec. Such geometrical conditions as the channel width, height and liquid depth were the same as the previous numerical prediction that was computed without internal heating. The intensity of the internal heating was  $\dot{q} = 47 \text{ W/mm}^3$ . The surface temperature, in contrast, was set to the same value with initial temperature of liquid. The Rayleigh number of internal heating, which is defined as  $Ri = g\beta qL^5/k\nu\alpha$  was  $7.3 \times 10^7$ .



**Figure 3:** Temporal profile of the temperature in the cavity. Representative 4 points were depicted.

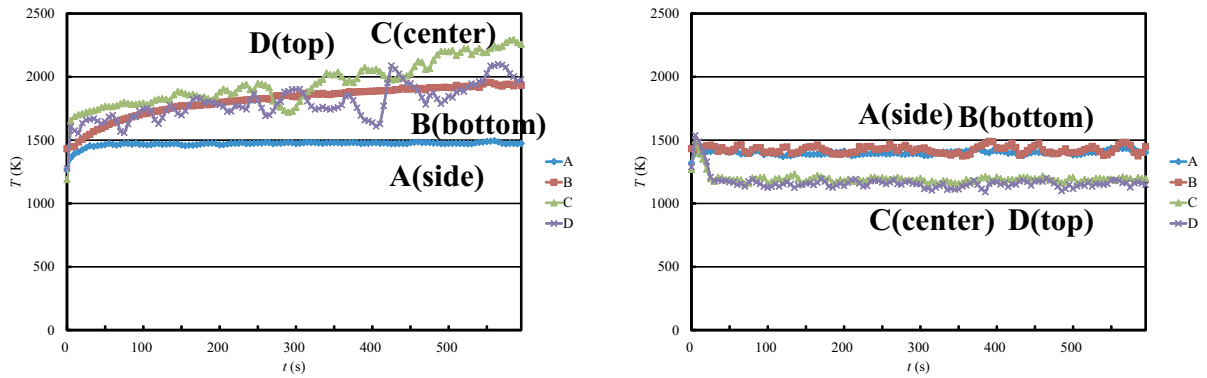
Figure 3 compares the temperature profile without an internal heating. Temperature transition at the representative four points were depicted. Due to the constant boundary condition of temperature, the temperature in the vicinity of the bottom surface, which corresponds to the point A and B, is rapidly increased and reached to the surface temperature. The temperatures at the other two points, which were located in the fluid flow, increased with some delay due to the conductive heat transfer. After several ten seconds, the large-scale vortex was induced that accelerated the heat transfer within a cavity.

Figure 4 shows an instantaneous colour contour of the temperature field with an internal heating. At the beginning of the internal heating, temperature of liquid was homogeneously increased. The convection pattern becomes different especially near the vertical walls due to the constant lower temperature of the wall. In contrast to the velocity distribution by the wall heating, a pair of vortex is appeared at the vertical surface with downward flow in the vicinity of the vertical surface. Since the fluid flow was heated due to the internal heating, the difference of fluid velocity was observed due to the inverse temperature gradient at the vertical surface. After the several ten seconds, the magnitude of fluid velocity was decreased since the temperature difference between solid wall and fluid flow was decreased. With the steady state under which the energy supply due



**Figure 4:** Colour contour map of the temperature field of the internally heated cavity. Unsteady downward plumes were appeared in the vicinity of the surface.

to the internal heating and cooling by the wall was balanced, only the stable and weak convection is appeared in the vicinity of the both vertical surfaces.



**Figure 5:** Comparison of temperature profile over time in terms of the heat flux at the surface. Higher surface heat transfer rate stabilise the internal temperature field. Heat trans fed rate at the free surface was varied, lower heat flux(left), larger thermal energy transport(right).

Figure 5 is the comparison of temperature fluctuation under the different intensity of the heat transfer at the free surface. Under the lower thermal energy transport at the interface, the liquid temperature at the pint C and D were continuously increased that will damage the cavity substrate. Moreover the degree of the temperature fluctuation is beyond 400 degree. In contrast, the higher heat transfer rate such as the evaporation at the surface could stabilise the overall temperature within a cavity due to the convection of the fluid flow. The amplitude of the temperature fluctuation could be suppressed below 100 degree.



## 4 Conclusions

Natural convection in a two-dimensional rectangular cavity with internal heating was predicted by means of particle method. Under the internal heating condition, the flow structure was significantly governed by buoyancy as well as viscosity. It is considered that the field with the vertical temperature gradient due to the homogeneous internal heating is essentially stable under the present dimensionless number. The thermal boundary layer in the vicinity of the vertical surface induces the characteristic downward flow at the both edge of a cavity, the resultant magnitude of the velocity was  $10^{-3}$  m/s approximately in the present configuration. By controlling the surface heat flux, the resultant molten glass temperature could be stabilised below the solid wall temperature.

## Nomenclature

$c_p$	Specific heat
$g$	Gravitational acceleration
$k$	Thermal conductivity
$l_0$	Initial particle-particle distance
$n$	Coefficient for viscosity
$q$	Internal heating energy
$r$	Inter-particle distance
$r_e$	Particle radius
$v$	Velocity
$D$	Strain rate tensor
$P$	Pressure
$T$	Temperature
$\alpha$	Thermal diffusivity
$\beta$	Volume expansion coefficient
$\eta$	Coefficient for viscosity
$\nu$	Kinematic viscosity
$\rho$	Density
$\tau$	Shear stress

## REFERENCES

- [1] Turcotte, D.L. and Schubert, G. (2001) *Geodynamics 2nd edition*, Cambridge Univ. Press
- [2] Stanek, J., Sasek, L. and Meissnerova, H. (1969) Flow of glass in furnaces heated by electricity, *Glass Technology* **10**, 2, 43–49
- [3] Roberts, P.H. (1967) Convection in horizontal layers with internal heat generation. Theory, *J. Fluid Mech.*, **30**, 1, 33–49

- [4] Tritton,D.J. and Zarraga,M.N. (1967) Convection in horizontal layers with internal heat generation. Experiments, *J. Fluid Mech*, **30**,1, 21–31
- [5] Tveitereid,M. (1978) Thermal convection in a horizontal fluid layer with internal heat source, *Int. J. Heat and Mass Transfer*, **21**, 335–339
- [6] Gurnis,M. and Davis,G.F. (1985) Numerical study of high Rayleigh number convection in a medium with depth-dependent viscosity, *Geophys. J. R. astr Soc.*, **186**, 523–541
- [7] Char,M.I. and Chiang,K.T. (1994) Stability analysis of Benard–Marangoni convection in fluids with internal heat generation, *J. Phys. D: Appl. Phys.*, **27**, 748–755
- [8] Liaqat,A. and Baytas,A.C. (2000) Heat transfer characteristics of internally heated liquid pools at high Rayleigh numbers, *Heat and Mass transfer*, **36**, 401–405
- [9] Kawaguchi, T. (2011) Experimental investigation of natural convection with internal Joule heating in a rectangular cavity, *9th international symposium on particle image velocimetry*, CDROM, Kobe, Japan.
- [10] Kawaguchi,T., Saito,T. and Satoh,I. (2012) Experimental analysis of natural convection with Joule heating by means of particle image velocimetry *16th Int Symp on Applications of Laser Techniques to Fluid Mechanics*, CDROM, Lisbon, Portugal.
- [11] Kawaguchi, T. (2011) Natural convection in a rectangular cavity with internal heating by particle method, *The asian symposium on computational heat transfer and fluid flow*, CDROM, Kyoto, Japan.
- [12] Koshizuka,S., Ikeda,H. and Oka,Y. (1999) *Nuclear Engineering and Design*, **189**, 1–3, 423–433
- [13] Hottel,H.C. and Sarofim,A.F. (1967) *Radiative Transfer*, McGraw-Hill,